



## Efectos producidos por los huecos de tensión reales en un motor de inducción

### Effects produced by real sags on an induction motor

Juan Camilo Urrego García<sup>1</sup>, Wilmar Camilo Molina Gómez<sup>2</sup>,  
Adolfo Andrés Jaramillo Matta<sup>3</sup>

**Fecha de recepción:** Agosto 28 de 2015

**Fecha de aceptación:** Septiembre 25 de 2015

**Como citar:** Urrego, J., Molina, W., & Jaramillo, A. (2015). Effects produced by real sags on an induction motor. Revista Tecnura, 19 (CITIE), 157-163. doi: 10.14483/udistrital.jour.tecnura.2015.ICE.a0

#### Resumen

En este artículo se analizan los efectos de los huecos de tensión reales en el comportamiento del motor de inducción. Para ello se desarrolla el modelo matemático de un motor de inducción trifásico, se modelan los huecos de tensión reales variando los parámetros de profundidad y duración con el fin de someter el motor de inducción una gran cantidad de huecos de tensión y por último se presenta el análisis de los resultados obtenidos. Los análisis se enfocan sobre las variables de picos de corriente y picos de par, se determina una clasificación por grupos de severidad de los efectos en función de la tipología del hueco y la variable analizada.

**Palabras claves:** Distancia euclídea; Grupos de severidad; Modelos de huecos reales; Modelo del motor de inducción; Picos de corriente; Picos de par.

#### Abstract

This paper analyzes the effects of real voltage sags in the behavior of an induction motor. The mathematical model of a three phase induction motor is developed, the real voltage sags are modeled varying the depth and duration parameters to subject the induction motor to a large samples of voltage sags. Current peaks and torque peaks are analyzed and classified on a group of severity based on effects produced by sag typology.

**Keywords:** Euclidean distance; Group of severity; Real sag model; Induction motor model; Current peaks; Torque peaks.

<sup>1</sup> Estudiante de Ingeniería Eléctrica, Universidad Distrital Francisco José de Caldas, Bogotá D.C., Colombia. Contact: [jcurreregog@correo.udistrital.edu.co](mailto:jcurreregog@correo.udistrital.edu.co).

<sup>2</sup> Estudiante de Ingeniería Eléctrica, Universidad Distrital Francisco José de Caldas, Bogotá D.C., Colombia. Contact: [wcmolinag@correo.udistrital.edu.co](mailto:wcmolinag@correo.udistrital.edu.co).

<sup>3</sup> Ingeniero Electrónico, Magister en Ingeniería Electrónica, Magister en Ingeniería-Énfasis en Automática, Doctor en Ingeniería Electrónica, Automática y Comunicaciones, Bogotá D.C., Colombia. Contact: [ajaramillom@udistrital.edu.co](mailto:ajaramillom@udistrital.edu.co).

## INTRODUCTION

Currently, energy quality is an interesting topic due to the effect that electric disturbs cause in electrical systems. Sags are identified as a fall of voltage signal with short duration. Due to their frequent presence on electrical systems their severity could be worse than other kind of disturbances in electrical network.

It is well known that induction machine belongs to almost 80% of electrical industrial loads due to its special electrical and mechanical characteristics (Hedayati & Mariun, 2012). Induction motor is very sensitive to sags voltage disturbances. In fact, it is necessary to understand the behavior that induction motor will have when it is subjected by voltage disturbance sags.

Many studies and researches have been carried out to assess, satisfy and enhance the power quality effects in induction motor, however the most of sag contribution studies develop models based on ideal sags that in most cases do not represent real scenarios of sags effects. Features as presence of delay in the voltage recovery after the fault is cleared, fall slope, recover slope and peaks of short duration are ignored when ideal sags are used in the simulation of electrical systems. It is wrong to not include such parameters because the excessive voltage drop due to the feeder impedance prevents fast recovery of the internal electromagnetic forces of motor (Aree, 2012). The effects caused by real sags on the motor dynamics are discussed in this paper.

## METHODOLOGY

### Induction machine model

The selected induction motor model is the single cage, and for the estimation of its parameters the technique in (Jaramillo-Matta, 2010) is used, this technique, called torque-speed tracking, begins with manufacture data and solve issues caused by missed functional points given by manufacturer.

### Modeling sags

The real sags not consider a pattern easy to identify, they have different features of waveform, duration and depth. Real sags present different magnitudes before, during and after fault happen, they are not rectangular. Modeling a sag by ideal path involves loss of information because effects produced by voltage sags are closely related to the way that voltage drop on each phase (García-Quintero, Villada-Duque, & Cadavid-Carmona, 2011).

### Effects of real sags on induction motor

Current peaks and torque peaks studies exposed that induction motor effects are very sensitive to short interruptions and voltage sags (Bollen, Hager, & Roxenius, 2003; Guasch, Corcoles, & Pedra, 2000, 2004; Pedra, Sainz, & Córcoles, 2007). Current peaks and torque peaks are analyzed and classified on a group of severity based on effects produced by sag typology. A distance from peaks-duration-depth 3D surfaces to maximum peaks surfaces is calculated to obtain the most severe effects caused by each sag type.

### Procedure

The normalized distances (D) between surfaces of current peaks and torque peaks generated by real sags are calculated as follows:

$$d(I_X, I_Y) = \frac{100}{D_{REF,I}} \sqrt{\sum_{i=1}^{25} \sum_{j=1}^{25} [I_X(i,j) - I_Y(i,j)]^2} \quad (1)$$

$$d(\Gamma_X, \Gamma_Y) = \frac{100}{D_{REF,\Gamma}} \sqrt{\sum_{i=1}^{25} \sum_{j=1}^{25} [\Gamma_X(i,j) - \Gamma_Y(i,j)]^2} \quad (2)$$

Where X can be the surface of typology corresponding to the sag analyzed (A, B, C, D, E, F, G), Y can be the surface of typology corresponding to the sag analyzed (A, B, C, D, E, F, G) but also can be the surface of maximum values for each variable (IMAX,  $\Gamma$ MAX). The surface of maximum values is used as Reference in order to calculate the distance to be analyzed.

As an example, Figure 1 shows the surface of Maximum values of all current peaks (Reference surface) and the current peaks surface caused by voltage sags type G.

The distance between the surfaces in Figure 1 is calculated as in the equation (1) and the result is 43.959%.

In Figure 2 is shown the torque peaks surface caused by voltage sags type B. In this case the distance between the surfaces is 35.443%, and is calculated as in the equation (2).

## RESULTS

### Induction machine model

For construction of electromechanical mode damping, the linearized model around nominal operation is commonly used. The specifications of selected induction machine are as follows:  $P=75\text{kW}$ ,  $V_L=3,3\text{kV}$ , frequency= $50\text{ Hz}$ ,  $n_m=1455\text{ r/min}$ .

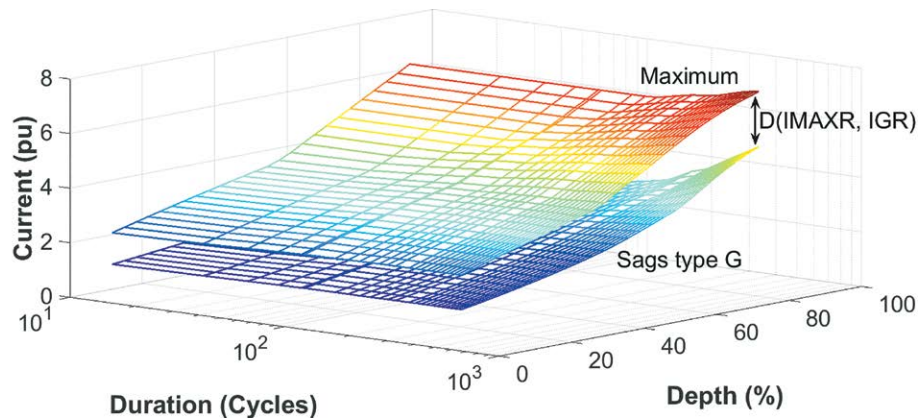


**Figure 1.** Surface of Maximum values of all current peaks and surface of current peaks caused by sags type G.

Source: own work

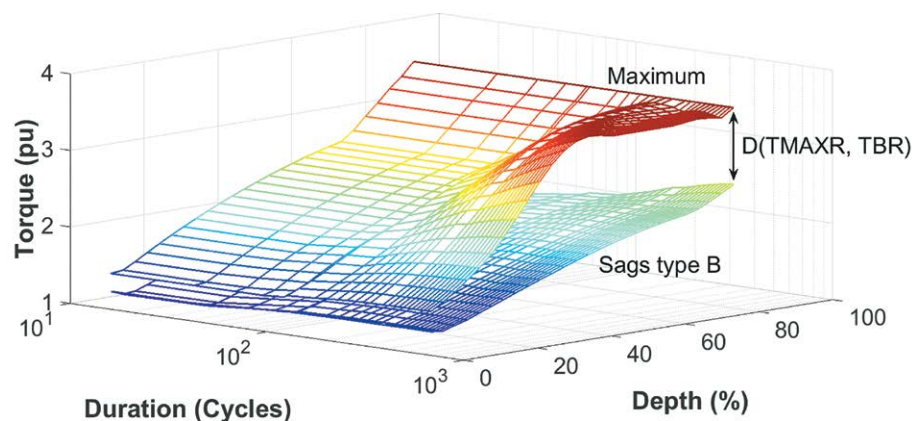


**Figure 2.** Surface of Maximum values of all torque peaks and surface of torque peaks caused by sags type B.

Source: own work

Induction machine model used is showed in Figure 3; also electrical parameters calculated by torque-speed tracking are depicted in Table 1.

**Table 1.** Parameters estimated by Torque-Speed Tracking technic (Jaramillo-Matta, 2010).

P (KW)	$r_s$	$X_{sd}$	$X_m$	$X_{rd}$	$r_r$
75	0,098	0,155	4,127	0,155	0,077

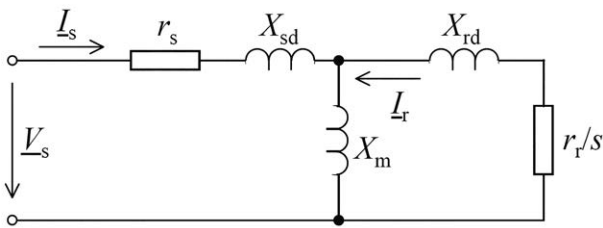


**Figure 3.** Steady state equivalent circuit of induction machine (Pesquer, 2006).

The equations that represent electrical behavior of induction machine are:

$$[v] = [R][i] + \frac{d}{dt} [\phi] \quad (3)$$

$$\begin{bmatrix} v_s \\ v_r \end{bmatrix} = \begin{bmatrix} R_s & 0 \\ 0 & R_r \end{bmatrix} \begin{bmatrix} i_s \\ i_r \end{bmatrix} + \frac{d}{dt} \begin{bmatrix} \phi_s \\ \phi_r \end{bmatrix} \quad (4)$$

The ratio among magnetic fluxes and currents is:

$$\begin{bmatrix} \phi_s \\ \phi_r \end{bmatrix} = \begin{bmatrix} M_{ss} & M_{sr} \\ M_{rs} & M_{rr} \end{bmatrix} \begin{bmatrix} i_s \\ i_r \end{bmatrix} \quad (5)$$

Understanding that the  $M_{sr}$  matrix (coupling coefficient matrix of the flow created by the rotor windings and concatenated by the stator coils) is equal to the  $M_{rs}$  Matrix (coupling coefficient matrix of the streams created by the stator coils and concatenated to the rotor windings), it leads to the torque equation (6):

$$\Gamma(t) = [i_s]^t \left\{ \frac{\partial}{\partial \theta} [M_{sr}(\theta)] \right\} [i_r] \quad (6)$$

Due to the dependency of equation (6) with  $\theta$ , workload-calculating time would increase, and it cannot be calculated if basic methods of differential equation solution are used. To solve this problem, the Ku transformation is implemented (Bort, 2002) to convert complex and variable coefficient into lineal constants coefficients.

### Real sag model

Modeling a real sag by mathematical function with polynomial regression technique would suppose a loss of important information, to illustrate this, Figure 4 shows a real sag and it approximation

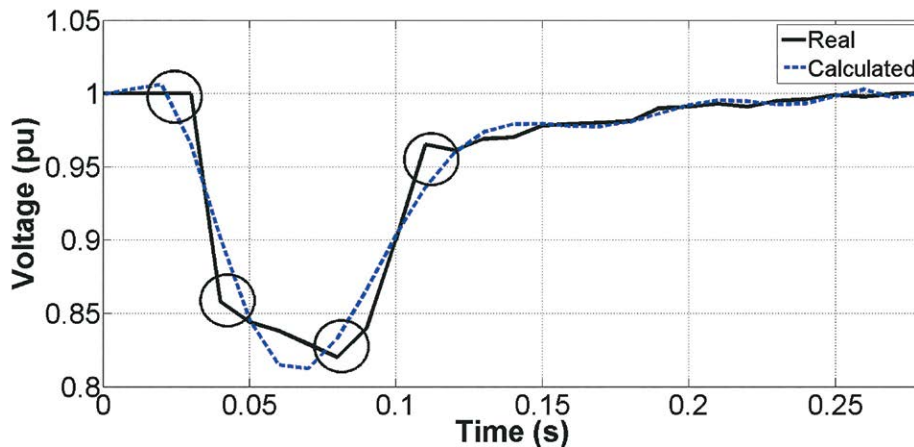


**Figure 4.** Mathematical sag model obtained from 50 grade polynomial regression and sag measured by signal analyzer.

Source: own work.

(calculated) by 50 grade polynomial regression using the polyfit() function of Matlab, however features as fall slope, recover slope, minimum descent point and start point change from real model to mathematical expression.

To avoid this issue, the model is obtained by electrical signal analyzer with resolution of 0.833ms; an interpolation technique was applied to obtain 200 samples per cycle. From 12 three-phase real sag samples within different magnitudes, durations and shapes, 7500 real sags were obtained.

### Effects of real sags on induction motor

The effects need to be measured, the procedure consist on calculation of distance from surfaces generated by real sags, for each sag topology, on the

variables current peaks and torque peaks obtained in simulations. Overall results can be checked in follow items:

#### Current peaks

The sags type E obtain the less distance from maximum peaks surface reaching the 9.9%, in other side the sags type G present the longest distance among other sags typologies being those last one the less severe. Results can be checked in Table 2.

#### Torque peaks

The sags type A, D, F and E have the minor distance from maximum peaks surface, their distance vary from 12% to 20%. The minor distance is obtained with sags type A which distance reach the 12.6%, being this one the most severe as Table 3 shows.

**Table 2.** Normalized distances between peak current surfaces obtained by real voltage sag

Real (% PU) Real (% PU)	IA	IB	IC	ID	IE	IF	IG	IMax
IA	0	21.208	25.563	20.005	29.683	27.006	19.629	33.597
IB	21.208	0	25.075	2.7300	28.301	17.296	15.144	32.760
IC	25.563	25.075	0	22.798	18.006	20.846	33.403	15.799
ID	20.005	2.730	22.798	0	26.308	15.946	16.060	30.782
IE	29.683	28.301	18.006	26.308	0	13.761	39.930	9.9723
IF	27.006	17.296	20.846	15.946	13.761	0	31.079	20.164
IG	19.629	15.144	33.403	16.060	39.930	31.079	0	43.959
IMax	33.597	32.760	15.799	30.782	9.9723	20.164	43.959	0

Source: own work.

**Table 3.** Normalized distance between torque peaks for real voltage sags.

Real (% PU) Real (% PU)	IA	IB	IC	ID	IE	IF	IG	IMax
IA	0	33.6457	31.0546	21.2939	17.4724	21.8717	21.5440	12.688
IB	33.6457	0	6.8554	18.7728	20.4888	22.5843	18.2089	35.443
IC	31.0546	6.8554	0	19.7202	18.4182	22.8597	15.8595	34.905
ID	21.2939	18.7728	19.7202	0	13.8209	10.8573	15.1305	18.941
IE	17.4724	20.4888	18.4182	13.8209	0	11.3669	4.6955	20.963
IF	21.8717	22.5843	22.8597	10.8573	11.3669	0	12.3881	19.008
IG	21.5440	18.2089	15.8595	15.1305	4.6955	12.3881	0	25.058
IMax	12.688	35.443	34.905	18.941	20.963	19.008	25.058	0

Source: own work.

The sags type C and B presented the mayor distance therefore their effects are the less severe.

### Severity groups

The severity of the effects is compared among sag typologies based on effects on current peaks and torque peaks. An induction motor is subjected to all variation of sags designed, results are classified in Table 4 where severity is categorized in three levels: high, medium and low.

**Table 4.** Severity of voltage sags for current peaks ( $I_p$ ), torque peaks ( $T_p$ ) for real voltage sags.

Variable Severity	$I_p$	$T_p$
High	E	A
Medium	C, F A, B, D	D, E, F, G
Low	G	B, C

**Source:** own work.

When motor is analyzed with real sags, the most severe effects in current peaks are obtained with sags type E, the less severity is obtained with sags type G.

In other studies it has previously studied the ideal voltage sags effects in an induction motor (Alejandro Diego Jurado, 2010; Andreia Leiria, Pedro Nunes, & Barros, 2003; Aree, 2012; Bollen et al., 2003; Jaramillo-Matta, 2010, 2013; M.G. Macri, 2012; Pesquer, 2006), a quick analysis shows that it is possible that the effects on speed behavior of the induction motor are very similar, when the analysis is done with real and ideal sags. On the other hand, a big difference could be that the current and torque peaks happens at the beginning and in the end of ideal sags but these peak happens in other time during a real sag. However this analysis is out of the scope of this paper, due to the comparison of the effects of real and ideal sags

on the induction motors needs a deeper analysis with particular characteristics.

### CONCLUSION

In this paper the effects of real sags on single cage induction motor were obtained, analyzed and classified. An algorithm was designed to observe changes presented in current peaks and torque peaks of induction motor based on type, duration and depth of real sag.

The effects obtained by sags type E were the most severe on current variable, they are harmful to motor because thermal stress produced exceeds the operating conditions suggested by manufacturer. The sags type G produced the less effects on current peaks.

The effects produced by sags type A on torque are considered the most severe according to it generated surfaces which are close to maximum peaks surface, whereas the surfaces generated by sags type B and C presented the mayor distance so their effects are the less severe. In almost all cases the peaks of current and torque are presented during sag perturbation, once it ends, the signal returns to normal values.

### FINANCIAMIENTO:

Universidad Distrital Francisco José de Caldas

### REFERENCES

- Alejandro Diego Jurado, N. A. L. (2010). Efecto de los huecos de tensión en el motor de inducción. *Grupo Energía y Ambiente. Facultad de Ingeniería. Universidad de Buenos Aires.*
- Andreia Leiria, Pedro Nunes, & Barros, A. M. a. M. T. C. d. (2003). Induction Motor Response to Voltage Dips. *International Conference on Power Systems Transients – IPST 2003 in New Orleans, USA.*
- Aree, P. (2012, 27-29 March 2012). *Effects of Large Induction Motors on Voltage Sag.* Paper presented

- at the Power and Energy Engineering Conference (APPEEC), 2012 Asia-Pacific.
- Bollen, M. H. J., Hager, M., & Roxenius, C. (2003, 23-26 June 2003). *Effect of induction motors and other loads on voltage dips: theory and measurements*. Paper presented at the Power Tech Conference Proceedings, 2003 IEEE Bologna.
- Bort, J. V. (2002). *Estudio del Modelo Matemático del Motor de Inducción Trifásico*. UNIVERSITAT ROVIRA I VIRGILI.
- García-Quintero, E., Villada-Duque, F., & Cadavid-Carmona, D. (2011). Nuevo factor para la caracterización de huecos de tensión. *Revista Facultad de Ingeniería Universidad de Antioquia*, 59, 12.
- Guasch, L., Corcoles, F., & Pedra, J. (2000, 2000). *Effects of unsymmetrical voltage sag types E, F and G on induction motors*. Paper presented at the Harmonics and Quality of Power, 2000. Proceedings. Ninth International Conference on.
- Guasch, L., Corcoles, F., & Pedra, J. (2004). Effects of symmetrical and unsymmetrical voltage sags on induction machines. *Power Delivery, IEEE Transactions on*, 19(2), 774-782. doi:10.1109/TPWRD.2004.825258
- Hedayati, M., & Mariun, N. (2012, 15-16 Feb. 2012). *Assessment of different voltage sags on performance of induction motors operated with shunt FACTS*. Paper presented at the Power Electronics and Drive Systems Technology (PEDSTC), 2012 3rd.
- Jaramillo-Matta, A. A. (2010). ESTIMACIÓN DE PARÁMETROS Y EFECTOS DE LOS HUECOS DE TENSIÓN EN LA MÁQUINA DE INDUCCIÓN TRIFÁSICA. *UNIVERSITAT ROVIRA I VIRGILI*.
- Jaramillo-Matta, A. A. (2013). Efecto de las perturbaciones: huecos de tensión, desequilibrios de tensión y armónicos, en los motores de inducción con rotor Jaula de Ardilla. *Universidad Antonio Nariño—Revista Facultad de Ingenierías*, 4, 36-51.
- M.G. Macri, M. B. (2012). Análisis multirresolución del motor trifásico de inducción sometido a huecos de tensión. *Ingeniare. Revista chilena de ingeniería*, 20, 66-78. Retrieved from [http://www.scielo.cl/scielo.php?pid=S0718-33052012000100007&script=sci\\_arttext](http://www.scielo.cl/scielo.php?pid=S0718-33052012000100007&script=sci_arttext)
- Pedra, J., Sainz, L., & Córcoles, F. (2007). Effects of symmetrical voltage sags on squirrel-cage induction motors. *Electric Power Systems Research*, 77(12), 1672-1680. doi:<http://dx.doi.org/10.1016/j.epsr.2006.11.011>
- Pesquer, L. G. (2006). Efectos de los huecos de tensión en las máquinas de inducción y en los transformadores trifásicos. *Universitat Politècnica de Catalunya Department d'Enginyeria Elèctrica*.